Modeling the Dual Nature of Ionizing Radiation: Analyzing DNA Double-Strand Break Repair Using Differential Equations Approach

¹Mustapha Mohammed Karagama, ²Fuaada Mohd Siam*, ²Norma Alias and ³Dalal Yahya Alzahrani

Department of Mathematics, Faculty of Physical Sciences, University of Maiduguri,
Borno State, Maiduguri, Nigeria.
 Department of Mathematical Sciences, Faculty of Science, Universiti Teknologi Malaysia,
81310 UTM Johor Bahru, Johor, Malaysia.
 Department of Mathematics, Faculty of Science, Al Baha University,
Al Bahah, 65528, Saudi Arabia.
 *Corresponding author: fuaada@utm.my

Article history

Received: 19 November 2024

Received in revised form: 22 March 2025

Accepted: 23 April 2025

Published online: 15 November 2025

Abstract The term "dual nature of ionizing radiation" effectively describes the complex effects of irradiation on human cells. This study investigates how radiation affects the structural integrity of DNA, with a specific focus on double-strand breaks (DSBs). The primary objective was to enhance the existing model of bystander effects by allowing for the concurrent repair of multiple DSBs, thus improving our understanding of how cells respond to radiation. To accomplish this, we employed the exponential matrix method to solve a system of ordinary differential equations (ODEs) using MATLAB R2024a. The refined model provides a detailed representation of cell populations and DNA damage, explicitly incorporating the number of DSBs and incorrectly repaired breaks. Unlike previous models, this new approach takes into account the simultaneous repair of multiple DSBs, offering a more biologically realistic depiction of cellular repair dynamics. Simulation results indicate a 37% improvement in cell survival fractions compared to the existing model. Additionally, we validated the model predictions against experimental survival fraction data, demonstrating a strong agreement that confirms the model's reliability in assessing radiation-induced cellular responses. Future work could explore alternative methods for solving ODEs and integrate cell cycle parameters to further enhance the model's accuracy. These insights contribute to a deeper understanding of DNA repair mechanisms, paving the way for innovations in radiation biology and therapeutic strategies.

Keywords Irradiation, Structured ODE Model, Double Strand Breaks repair, Linear Quadratic, Exponential Matrix.

Mathematics Subject Classification 90C20, 92D25, 92C50, 92C37.

1 Introduction

The damage inflicted on deoxyribonucleic acid (DNA) activates crucial repair mechanisms and signaling pathways, which ultimately lead to cell-cycle arrest and, in severe cases, cell death [1]. Human cells exposed to radiation typically suffer from double-strand breaks (DSBs) along their chromosomal arms. These chromosomal abnormalities can disrupt chromosome arrangement, significantly increasing the risk of cancer development [2]. Insights from this study can contribute to radiation protection guidelines and personalized oncology treatment, enhancing patient safety [3]. In addition, our knowledge of DNA repair dynamics improved in this research, can help optimize radiation doses in radiotherapy, reduce harm to normal tissues, and enlighten the development of drugs that modulate DNA repair [4]. Furthermore, advancing cancer treatment and radiotherapy requires a crucial understanding of these mechanisms [5]. To better understand the cellular response to irradiation, researchers have employed various mechanistic models [6]. The term "mechanistic" refers to models grounded in physical, chemical, and biological principles that simulate complex biological responses to radiation by incorporating fundamental processes such as DNA repair and cell survival [7]. The study of radiation-induced DNA damage and repair is essential for understanding how cells respond to ionizing radiation (IR), which has implications for radiotherapy and radioprotection [8]. Various modeling approaches have been used to explore these processes, including differential equations, stochastic and agent-based models [8], Monte Carlo simulations [9], 3D genome organization [10], organoid models [11], and machine learning [12]. Among these, differential equation models are particularly popular due to their ability to describe the temporal evolution of DNA repair and survival processes. They offer a mathematically robust framework that can integrate various biological factors to predict how cells respond to radiation [13]. The foundational model that emerged from the target model theory posits dual irradiation action [14]. This concept asserts that the DSBs (sublesions) arising from eukaryotic irradiation are proportionate to radiation exposure. When two DSBs occur in a sensitive region, they can interact, forming a lesion that is classified as a fatal chromosomal abnormality. This duality of irradiation action is based on microdosimetry principles, which analyze energy distribution resulting from both direct and indirect irradiation, thus leading to bystander effects [15]. Microdosimetry is employed to understand the effects of radiation at the cellular and subcellular level by studying energy deposition at a microscopic scale, especially in biological targets [16].

By stander effects describe a series of responses that occur in non-irradiated cells, triggered by signals from their irradiated neighbors [17]. Several studies have demonstrated that these effects can induce DNA damage, apoptosis, or altered gene expression in nearby cells, even without direct radiation exposure [18]. [19] elaborates on this by stating that these effects instigate biological changes in nearby, non-irradiated cells, which may include stress responses, genomic instability, and modifications in cellular communication pathways [20]. Furthermore, [21] characterizes by stander effects as physiological responses that exceed expected radiation impacts, typically driven by reactive oxygen species (ROS) and cytokines. ROS can lead to oxidative stress, causing DNA strand breaks and mitochondrial dysfunction [22], while cytokines such as TNF- α , IL-6, and TGF- β have been shown to amplify inflammatory responses and influence DNA repair pathways [23]. Such effects can occur locally between adjacent cells or manifest as cohort effects, including vascular remodeling and intensified immune responses [24]. Supporting this notion, [25] cites data from medium transfer experiments, revealing that substances released by irradiated cells can significantly affect non-irradiated counterparts. This interaction is facilitated by the release of soluble molecules and exosomes, which mediate intercellular signaling and contribute to DNA damage propagation [26] DNA can suffer damage from a variety of sources, which include both direct and indirect irradiation [27] Chargedparticle radiation, due to its high energy, can disrupt atomic structures and induce chemical and biological alterations (direct irradiation). Conversely, indirect damage occurs through the generation of highly reactive free radicals. The oxidative damage that DNA incurs arises from the interactions between DNA and free radicals, leading to structural abnormalities [28]. Additionally, created a model that effectively depicts the effects of DNA DSBs on the survival of mammalian cells following irradiation, both direct and indirect. Moreover, [27] employed IR alongside anti-programmed death ligand 1 (PD-L1) therapies to investigate tumor development, utilizing a simplified ordinary differential equation (ODE). However, this study aims to modify the existing bystander effects model presented by [15] to simultaneously repair three DSBs. Recognizing DSBs as the most critical form of radiation-induced DNA damage is essential. Understanding these irradiative impacts on cellular structures is crucial, as they lead to significant DNA damage commonly referred to as DSBs. If left unrepaired, DSBs can result in a variety of health issues, including cell death, genomic instability, chromosomal aberrations, sister chromatid exchanges, mutations, and ultimately cancer. Therefore, rectifying DNA damage stemming from DSBs is of utmost importance. This study is dedicated to modifying the existing model to facilitate the concurrent repair of three DSBs.

This concept draws inspiration from [29], who examined the current landscape of mathematical biology, arguing that researchers have become overly focused on evaluating existing models instead of innovating new ones. This methodology champions a pluralistic approach to modeling biological systems, which emphasizes their inherent complexity and variability. The authors also highlight the influence of machine learning (ML) in the field, noting a concerning shift away from developing novel models. They advocate for researchers to place greater emphasis on creating and refining models that exhibit higher levels of originality within their respective scientific fields. Research indicates that DNA repair foci can simultaneously repair multiple DNA DSBs, supporting the idea that three DSBs can be repaired at once. This process involves repair proteins such as non-homologous end joining (NHEJ) and homologous recombination (HR) factors functioning within nuclear repair foci [30]. Studies like [31] have shown that DNA damage response (DDR) mechanisms are practiced at handling multiple DSBs simultaneously, particularly through chromatin remodeling and the strategic recruitment of repair protein. Furthermore, these processes are vital for maintaining genomic integrity, especially under conditions of severe DNA damage such as that caused by high-linear energy transfer (LET) radiation [32]. Similarly, emphasizes understanding these mechanisms provides insights into potential therapeutic strategies for enhancing DNA repair in cancer treatment. IR poses significant risks to human health by inflicting DNA damage. Research has demonstrated that exposure to IR leads to critical biological consequences, particularly DNA single-strand breaks (SSBs), DSBs, and base damage [28]. As noted by [33], these harmful effects encompass DSBs (k), and misrepair cells (m). DSBs are especially alarming; they occur when both strands of DNA are severed and cannot be adequately repaired, leading to misrepaired cells where chromosomes incorrectly fuse during the repair process [28]. To investigate these effects, the authors have introduced a structured population technique as a model for studying the consequences of IR exposure. Structured population models describe populations in which individuals are categorized based on specific attributes such as age, damage state, or cell cycle phase. These models allow for a more detailed evaluation of population dynamics under radiation exposure. This model specifically measures the quantities of DSBs and misrepaired cells in relation to the direct effects of irradiation. Given that DSBs are significantly more lethal than SSBs, the authors have rightly prioritized their examination of DSBs [28]. The implications of IR-induced DSBs on cell populations are profound, as they can lead to cell death. Furthermore, the level of radiation exposure plays a crucial role in determining the rate of DSB production [28]. This research highlights the urgent need to comprehend the mechanisms by which DNA damage and repair occur in response to IR. Understanding these processes is essential for accurately assessing the risks posed by radiation to human health, emphasizing the importance of continued study in this critical area.

To estimate the initial number of DSBs caused by radiation, we assume that their occurrence follows a Poisson distribution. This distribution is commonly used in radiobiology to describe random DNA damage events. In this study, the average number of DSBs, denoted as μ , is proportional to the radiation dose, D as expressed in Equation (1).

$$\mu = \delta D \tag{1}$$

In this study, δ refers to the radiosensitivity parameter, which determines the expected number of DSBs per unit of radiation dose. The probability of observing exactly k DSBs in a single cell can be expressed using the formula in Equation (2).

$$P(x = \text{no. DSBs} = k) = \frac{e^{-\mu}\mu^k}{k!}$$
 (2)

The parameter δ , which measures **radiosensitivity**, indicates the average number of DSBs induced per unit of radiation dose. This parameter is well-established in the field of radiobiology and is often estimated from experimental data gathered through cell survival curves and DNA damage assays. Numerous research studies have demonstrated that this parameter effectively characterizes the DNA damage response across various cell types, underscoring its significance in understanding cellular responses to radiation [33, 34].

The structured population model outlined in [33] serves as a mechanistic framework that uses the Linear Quadratic (LQ) formulation to calculate the mean value of the Poisson distribution, denoted as μ . This model is crucial for quantifying cell survival fractions over specified periods, particularly $\tau=24$ hours, which represents the maximum duration within the cell cycle. After exposure to IR, we examine the dynamics of DNA damage through a system of ODEs. This analysis incorporates essential factors such as repair rates, mortality rates, and the likelihood of successful DNA repair. To capture the time evolution of the cell population, we establish an ODE system that describes the number of cells in various states of DSBs (k) and misrepair (m). The governing equation considers three primary processes cell mortality resulting from radiation damage, repair of DSBs (k) via enzymatic processes, and misrepair (m) events that contribute to genomic instability. The governing equation is formulated in Equation (3).

$$\frac{dN_{k,m}}{d\tau} = -\beta_1(k,m)\boldsymbol{N}_{k,m}(\tau) - \kappa(k)\boldsymbol{N}_{k,m}(\tau) + P\kappa(k+1)\boldsymbol{N}_{k+1,m} + (1-P)\kappa(k+1)\boldsymbol{N}_{k+1,m-1}$$
(3)

 $N_{k,m}(\tau)$ represents the number of cells with k DSBs and m misrepaired DSBs at time τ . The term $\beta_1(k,m)$ indicates the mortality rate of cells due to radiation-induced damage, while $\kappa(k)$ is the repair rate function, defined in Equation (4) and (5) respectively.

$$\kappa(k) = \frac{V_{max}k}{K_M + k} \tag{4}$$

In this equation, V_{max} refers to the maximum repair rate, and K_M is the Michaelis constant, which corresponds to the saturation threshold for the repair rate. Conversely, the misrepair rate function is expressed in Equation (5):

$$\beta_1(k,m) = \alpha_1 m + \alpha_2 k^2 \tag{5}$$

Here, α_1 is a constant representing the misrepair rate, and α_2 reflects the probability of binary misrepair events occurring at two DNA strands. The probability of a successful repair is given in Equation (6). In contrast, the probability of an unsuccessful repair, which leads to misrepair, is represented in Equation (7). In this study, P represents the probability defined in Equation (3). This probability follows a Poisson distribution, which describes the likelihood of a specific number of DSBs occurring per cell after radiation exposure

$$P_{success} = P\kappa(k+1)\boldsymbol{N}_{k+1,m} \tag{6}$$

$$P_{failure} = (1 - P)\kappa(k+1)\boldsymbol{N}_{k+1,m-1} \tag{7}$$

This structured model provides a dynamic representation of DNA repair, enabling us to track how damage is processed over time. Equation (3) describes a system of linear first ODE that governs the evolution of $N_{k,m}(\tau)$. To solve this system, we utilize the matrix exponential method, which is commonly used for linear ODE systems of the form as shown in Equation (8)

$$\frac{d\mathbf{N}(\tau)}{d\tau} = \mathbf{A}\mathbf{N}(\tau) \tag{8}$$

In Equation (8), \mathbf{A} is the coefficient matrix that governs state transitions. The general solution to such a system can be expressed using the matrix exponential in Equation (9).

$$\mathbf{N}(\tau) = e^{\mathbf{A} \tau} \mathbf{N}(0) \tag{9}$$

Applying this approach to our structured population model, we derive the solution:

$$\mathbf{N}(\tau) = \mathbf{N}(0)e^{\mathbf{N}\tau} \tag{10}$$

The exponential term accounts for the cumulative effects of repair, misrepair, and mortality rates over time. The final solution to the system of ODEs determines the survival fraction and the proportion of cells that successfully repair or misrepair DSBs is expressed in Equation (10).

In this study, the matrix $N(\tau)$ illustrates the number of cells that successfully survived, informed by the initial conditions denoted by N(0) articulated through the Poisson distribution in Equation (2). The analysis of the ODE in Equation (3) involving the matrix N accounts for a critical time, τ , span of 24 hours, ensuring a comprehensive overview of the repair processes as indicated in [33]. Commencing this study, we outline the modifications made to the

mathematical framework surrounding the bystander effect phenomena, drawing from previous suggestions put forth by the author in [35]. The original mathematical modeling for the irradiation bystander effects, developed by [35], has important constraints, specifically its capacity to manage only one DSB repair or misrepair at a time and ignoring the complexities of the cell cycle. This study surpasses those limitations by modifying the existing model to support the concurrent repair or misrepair of up to three DSBs. While the current iteration does not incorporate the cell cycle, future research endeavors are aimed at seamlessly integrating this aspect. Our research is dedicated to refining the current model of bystander effect phenomena while executing comprehensive simulations [15,36]. The study is organized into four sections: the introduction provides an insightful overview and establishes the framework for ensuing modifications and assumptions. Section Two outlines the methodologies employed in this investigation, detailing the software utilized for the simulations. In Section Three, we present enlightening results and discuss their implications. Finally, in Section Four, we conclude by highlighting the critical significance of this innovative mathematical model, paving the way for further advancements in the field.

2 Method

In this section of the research, we will strategically utilize various methodologies introduced earlier in the study. To begin, we will calculate the initial number of DSBs present in the cell population using a Poisson distribution. With this information, we can construct a system of ODEs that accurately represents the dynamics of these DSBs. The complexity of the system will scale with the number of DSBs identified, enabling us to formulate a set of equations of order $n \times n$, (n = 136) tailored to our findings. We will then employ the exponential matrix method to solve this system of ODEs efficiently. Furthermore, to enhance our understanding and validation of the model, simulations will be carried out using MATLAB R2024a, ensuring robust and comprehensive results.

2.1 Mathematical Model

This section offers a compelling exploration of the mathematical model put forth by [35] to elucidate the irradiation bystander effect. The study employs a two-dimensional vector (k, m) to effectively represent a cell population, with one component indicating the number of DSBs (k) in each cell and the other, highlighting the number of DSBs that have been improperly repaired (m). Our focus is on a cell population that has been specifically exposed to a defined radiation dose, denoted as D. Following this exposure, a subset of cells referred to as N_k , 0(0), has encountered k DSBs, resulting in sustained damage. Importantly, this investigation emphasizes the significance of bystander cells, which are those that were not directly irradiated but can be influenced by damage occurring in adjacent cells. Thus,

$$\mathbf{N}(0) = \sum_{k=0}^{K_{max}} \mathbf{N}_{k,0}(0)$$
 (11)

The initial DSB load typically averages around this value:

$$S(0) = \frac{\sum_{k=0}^{K_{max}} k \mathbf{N}_{k,0}(0)}{\sum_{k=0}^{K_{max}} \mathbf{N}_{k,0}(0)}$$
(12)

where K_{max} denotes the maximum number of DSBs created in a particular cell population as a result of radiation exposure. The equation in (11) and (12) illustrating the progression of $N_{k,m}(\tau)$ over time, concerning a time interval $\Delta \tau$ is formulated as follows in Equation (13).

$$\mathbf{N}_{k,m}(\tau + \Delta \tau) = \mathbf{N}_{k,m}(\tau) - \Delta \tau \beta_1(k,m) \mathbf{N}_{k,m}(\tau) - \Delta \tau \sum_{n=1}^k \kappa(k,m,n) \mathbf{N}_{k,m}(\tau) + \Delta \tau \sum_{v=0}^m \sum_{u=1}^{u+v \le k_{max}-1} P(k+u+v,m-v,u,v) \\
\kappa(k+u+v,m-v,u,v) \mathbf{N}_{k+u+v,m-v(\tau)}$$
(13)

In Equation (13), the variables u and v represent the probabilities of success and failure, respectively. In this research, we define $N_{k,m}(\tau)$ as the cell population at time τ . The function $\beta_1(k,m)$ quantifies the death rate of cells affected by k DSBs and m mis-repaired DSBs. Meanwhile, $\kappa(k,m,q)$, characterizes the rate at which a cell with k DSBs and m mis-repaired DSBs repairs q DSBs concurrently, subject to the constraints $k \geq q$ and u+v=q, with u and v representing the counts of successful and unsuccessful repairs, respectively. Additionally, the probability that a cell repairs u DSBs successfully and v DSBs unsuccessfully within a unit time (τ) is expressed as P(k+u+v,m-1,u,v), where u+v must satisfy the condition $u+v \leq k_{max}-k$.

The function **repair rate** $\kappa(k) = \frac{V_{max}k}{K_M + k}$ follows a Michaelis-Menten-like kinetic framework is frequently employed in DNA repair studies to effectively models enzyme-mediated repair processes. This framework is supported by compelling evidence from research demonstrating saturation effects in DSB repair kinetics, particularly under high-damage conditions [34].

Besides, the equation death and misrepair rate $\beta_1(k,m) = \alpha_1 m + \alpha_2 k^2$ powerfully illustrates the dual impact of incorrect DNA end-joining (misrepair) and the destabilizing effects of multiple breaks on chromosomal integrity. The coefficients α_1 and α_2 are not arbitrary; they are grounded in experimental data that highlight the critical relationship between radiation-induced chromosomal aberrations and the improper rejoining of broken DNA strands. This connection underscores the importance of understanding misrepair rates in the context of genetic stability and the potential consequences for cellular function [37]. Thus, the repair rate function is intricately linked to the number of DSBs in the cell, which we denote as $\kappa(k)$. In this framework, we simplify $\kappa(k,m,q)$ to $\kappa(k)$ for clarity. The condition u+v=1 highlights two distinct scenarios: either one DSB is successfully repaired (with ((u+1)) and (v=0)), or one DSB fails to repair (where (u=0) and (v=1)). This comprehensive model enhances our understanding of DSB repair processes and underscores their critical implications for cellular survival. Therefore,

$$\mathbf{N}_{k,m}(\tau + \Delta \tau) = \mathbf{N}_{k,m}(\tau) - \Delta \tau \beta_1(k,m) \mathbf{N}_{k,m}(\tau) - \Delta \tau \kappa(k) \mathbf{N}_{k,m}(\tau) + \Delta \tau P(k+1,m,1,0) \kappa(k+1) \mathbf{N}_{k+1,m}(\tau) + \Delta \tau P(k+1,m-1,0,1) \kappa(k+1) \mathbf{N}_{k+1,m-1}(\tau)$$
(14)

The probability that a collection of cells with k+1 DSBs and m mis-repair DSBs can successfully repair one DSB is represented as P(k+1,m,1,0). On the other hand, the likelihood of this same group failing to repair one DSB, under the condition of having k+1 DSBs and m-1 mis-repair DSBs, is denoted as P(k+1,m-1,0,1). Importantly, it is assumed that every group of cells has an equal probability of effectively repairing a DSB, regardless of their total number of DSBs and mis-repair DSBs. This common probability is represented as P. Conversely, the probability of failing to repair one DSB is indicated as 1-P. Thus, as the limit of $\Delta \tau \to 0$, the linear structured ODE detailed in Equation (14) becomes more straightforward as shown in Equation (15).

$$\frac{d\mathbf{N}_{k,m}}{d\tau} = -\beta_1(k,m)\mathbf{N}_{k,m}(\tau) - \kappa(k)\mathbf{N}_{k,m}(\tau) + P\kappa(k+1)\mathbf{N}_{k+1,m} + (1-P)\kappa(k+1)\mathbf{N}_{k+1,m-1}$$
(15)

where $k = 0, 1, 2, ..., k_{max}$, $m = 0, 1, 2, ..., k_{max}$ with $k + m \le k_{max}$ and k_{max} is the maximum number of DSBs present in a population of cells. The cell survival curve, also known as the radiation survival curve, illustrates the relationship between radiation dose and the proportion of surviving cells, as shown in Figure 2. This curve provides insights into cellular radiosensitivity and the mechanisms that influence radiation response [28]. The Linear Quadratic (LQ) model is commonly used in radiobiology to describe the effects of ionizing radiation on cells and tissues. It quantifies the relationship between radiation dose and survival probability, aiding in the prediction of biological responses such as DNA damage and cell death, which may contribute to carcinogenesis [38]. To evaluate the accuracy of our modified model, we validated it against experimental survival data, as illustrated in Figure 4. The close alignment between the model's predictions and the experimental results confirms its reliability in estimating cell survival fractions after radiation exposure [39]. To quantify the effect of radiation on cell survival, we utilize the LQ model, to describe the relationship between radiation dose and cell viability. The survival fraction is expressed in Equation (16).

$$S = e^{-\alpha D - \beta D^2} \tag{16}$$

In Equation (16),S represents the fraction of cells that survive after receiving a specific dose D, while α and β signify constants that are determined based on empirical data [38]. The interaction of cell damage, which is proportional to both the dose and the square of the dose, achieves equilibrium as described in Equation (17). This equation is particularly useful in radiotherapy, as it enables predictions of cell survival across various radiation dose levels. By integrating our structured ODE model with the LQ formulation, we can evaluate the effectiveness of different DNA repair assumptions on long-term cell survival.

$$\alpha D = \beta D^2 \tag{17}$$

[40] states that the $\frac{\alpha}{\beta}$ ratio is a critical element in the LQ model, pivotal for evaluating tissue sensitivity to radiation treatment. This ratio indicates the balance between linear (α) and quadratic (β) components of radiation-induced damage. More specifically, the α component refers to the harm caused by a single ionizing event, whereas the β component pertains to the effects of two ionizing events, both contributing to cell death. As [40] highlights, the $\frac{\alpha}{\beta}$ ratio helps predict how different tissues respond to the fractionation used in radiotherapy. Higher ratios indicate cells or tissues are less sensitive to fractionation, suggesting they are less impacted by the number of treatment fractions, thereby aiding in the creation of optimal treatment schedules for enhanced therapeutic outcomes [37]. Additionally, biological repair mechanisms for DSBs can allow for the simultaneous repair of multiple DSBs. However, prior studies by [33,35] restricted their analyses to cases where only one DSB is repaired at a time. Furthermore, a study from [15] advanced the model to repair two DSBs concurrently but only stopped at the derivation stage, without performing simulation and empirical validation. In this study, we have refined the existing model to allow for the simultaneous repair of three DSBs, which enhances our understanding of DNA damage repair in radiobiology.

2.2 Modification of the Existing Model of the Bystander Effects Phenomena

The model of the bystander effects phenomenon presented in Section 2 (see Equation (11) and (14)) has been refined in this study. Our analysis focuses on the repair of a multiple DSBs with a defined probability (see Equation (18)) based on the fundamental assumptions of the existing framework:

$$u + v = q \tag{18}$$

where $u = P_{success}$ and $v = P_{failure}$ and q = 1.

This premise aligns with the probability theory outlined in [41], which confirms that the sum of all probabilities is always equal to one. Our aim is to convincingly demonstrate the logical viability of repairing one or more DSBs concurrently, thereby advancing our understanding of this complex biological process.

2.2.1 Possibilities of Repairing Single or Multiple DSBs at a Time

The probability framework governing DSB repair follows a structured pattern. When repairing n DSBs, there are n+1 possible outcomes, ensuring that all repair scenarios are accounted for.

For a single DSB (k = 1), there are two possible outcomes: complete success (u = 1, v = 0) or failure (u = 0, v = 1). These outcomes indicate either a successful or a not successful repair.

For two DSBs k=2, there are three possible outcomes: both successful (u=2,v=0), both failed u=0,v=2, or a mixed outcome u=1,v=1.

For three DSBs (k=3), there are four possible outcomes: all successful u=3, v=0, all failed u=0, v=3, or partial successes, which can be represented as either (u=2, v=1) or (u=1, v=2). Given this structured probability, the general form for repairing three DSBs is expressed as $u=P_{success}$, $v=P_{failure}$, and q=1 The potential repair outcomes can be categorized as correct or incorrect, as represented below.

$$\begin{cases} u, u, u \\ u, u, v \\ u, v, v \end{cases}$$
 Correct Scenarios
$$\begin{cases} v, v, v \\ v, v, u \\ v, u, u \end{cases}$$
 Incorrect Scenario
$$\begin{cases} v, v, v \\ v, v, u \\ v, u, u \end{cases}$$

While this framework allows for mathematical generalization to any n, where repairing n DSBs results in n+1 possible repair outcomes, we limit our model to repairing up to three DSBs because of the biological relevance of DNA repair foci generally process small clusters of DSBs, with efficiency decreasing as the complexity of the damage increases [28], computational feasibility of larger values of n introduce exponential complexity, making simulations impractical [37], and experimental data limitations of current research primarily focuses on small-scale DSB clusters [39]. Thus, our assumption balances mathematical generalizability with biological, computational, and experimental considerations, ensuring accuracy and applicability in radiation response modelling.

2.2.2 Existing Model

$$\frac{d\mathbf{N}_{k,m}}{d\tau} = -\beta_1(k,m)N_{k,m} + (1-P)\kappa(k+1)\mathbf{N}_{k+1,m-1}[37,38]$$
(19)

The probability term P(k+u+v,m-v,u,v) represents the likelihood of a group of cells transitioning from a state with DSBs and misrepaired DSBs to a new state following a repair attempt. In this expression k + u + v, denotes the updated total number of DSBs, considering additional breaks introduced during repair. The term m-v accounts for the adjusted number of misrepaired DSBs, reflecting successful repairs. Similarly, u represents successfully repaired DSBs, whereas v corresponds to failed repairs that contribute to misrepair. These transitions follow the constraints $0 < u + v \le k_{max} - k$ and u + v = q to ensure that each repair event aligns with a structured probability distribution. This formulation maintains biological realism, preserves the total number of DSBs, and accurately tracks the progression of misrepair. Therefore, P(k+u+v, m-v, u, v) serves as a mathematically consistent and biologically relevant model for the repair process. Previous models in Equation (19) only considered the repair of a single DSB per cell per unit time [15,36]. However, experimental evidence suggests that repair foci can simultaneously process multiple DSBs [42]. These repair clusters, known as radiation-induced foci (RIFs), contain essential repair proteins such as ATM, γ H2AX, and 53BP1, which can handle several DNA damage sites concurrently [42]. To incorporate this biological feature, we extend our model to allow for the concurrent repair of three DSBs. In this revised framework, we assume that a cell can repair up to three DSBs at the same time, assigning probabilities to different repair scenarios. Consequently, the governing equation is modified to include the sum of repair probabilities for one, two, or three DSBs per event. This leads to the following modified equation as expressed in Equation (20).

$$\frac{d\mathbf{N}_{k,m}}{d\tau} = -\beta_1(k,m)N_{k,m} - \kappa(k)\mathbf{N}_{k,m} + \sum_{n=1}^{3} P_n\kappa(k+n)\mathbf{N}_{k+n,m} + \sum_{n=1}^{3} (1-P_n)\kappa(k+n)\mathbf{N}_{k+n,m-n}$$
(20)

In Equation (20), P_n represents the probability of successfully repairing k DSBs simultaneously, where k can be 1, 2, or 3. This formulation takes into account biological observations of repair clusters handling multiple breaks at once, ultimately improving the accuracy of our model in predicting cell survival.

2.2.3 Modified Model

The biological mechanism that repairs DSBs is exceptionally efficient, enabling the simultaneous repair of multiple DSBs. This means that one or more DSBs can be repaired concurrently, showcasing the resilience of cellular repair systems. With parameters set at q = 1 and $\frac{u}{k} + \frac{v}{k} = 1$, the model operates within the defined constraints of $0 \le u, v \le k_{max} - k$. This flexibility allows for a robust and effective approach to managing DSB repair, illustrating the intricate capacity of biological systems to maintain genomic integrity. Therefore,

$$\kappa(k, m, q) = \kappa(k, m, 1) \tag{21}$$

The repair rate of a group of cells exhibiting k DSBs and m incorrectly repaired DSBs for the correction of three DSBs is expressed in Equation (21). It is important to note that this repair mechanism is specifically designed to tackle damage arising from DNA DSBs. As a result, the repair rate function is inherently tied to the number of DSBs present, meaning we can streamline $\kappa(k, m, 1)$ to simply $\kappa(k)$. The equation $\frac{u}{k} + \frac{v}{k} = 1$ highlights that our model accommodates two potential outcomes: either

u = 3, v = 0 or u = 2, v = 1 or u = 1, v = 2 (Successfully repairing three, two, or even one), or,

$$u=0, v=3$$
 or $u=1, v=2$ or $u=2, v=1$ (Unsuccessfully repairing three, two, or even one).

The two scenarios presented above are based on key assumptions from both the established models [36] and the newly proposed modified model. Notably, the modified model advances the assumption that three DSBs can be repaired, while the existing model recognizes only the repair of one DSB, as demonstrated in [33], and two DSBs, according to [15]. Crucially, the modified model retains all assumptions from the existing models along with those introduced in this study, creating a comprehensive framework for analysis. This is clearly articulated in Equation (28) and depicted in Figure (1), where parameters P_1 , P_2 , and P_3 effectively illustrate the critical differences between the frameworks.

$$\mathbf{N}_{k,m}(\tau + \Delta \tau) = \mathbf{N}_{k,m}(\tau) - \Delta \tau \beta_1(k,m) \mathbf{N}_{k,m}(\tau) - \Delta \tau \kappa(k) \mathbf{N}_{k,m}(\tau) + \Delta \tau P(k+u+v,m-v,u,v) \kappa(k+u+v) \mathbf{N}_{k+u+v,m-v}(\tau)$$
(22)

Equation (22) models the repair and misrepair of three DSBs but does not clearly differentiate between the various repair scenarios. To explain this, Equation (23) expands the probability terms to account for all possible repair outcomes: full repair of all three DSBs, complete misrepair, and mixed outcomes where one or two DSBs are repaired successfully while the others are misrepaired. This refinement creates a structured probability distribution that accurately represents all potential transitions in the repair process.

$$\mathbf{N}_{k,m}(\tau + \Delta \tau) = \mathbf{N}_{k,m}(\tau) - \Delta \tau \beta_{1}(k,n) \mathbf{N}_{k,m}(\tau) - \Delta \tau \kappa(k) \mathbf{N}_{k,m}(\tau) + \Delta \tau P(k+3,m,3,0) \kappa(k+3) \mathbf{N}_{k+3,m}(\tau) + \Delta \tau P(k+3,m-3,0,3) \kappa(k+3) \mathbf{N}_{k+3,m-3}(\tau) + \Delta \tau P(k+3,m-1,2,1) \kappa(k+3) \mathbf{N}_{k+3,m-1}(\tau) + \Delta \tau P(k+3,m-2,1,2) \kappa(k+3) \mathbf{N}_{k+3,m-2}(\tau) + \Delta \tau P(k+3,m-2,1,2) \kappa(k+3) \mathbf{N}_{k+3,m-2}(\tau) + \Delta \tau P(k+3,m-1,2,1) \kappa(k+3) \mathbf{N}_{k+3,m-1}(\tau)$$
(23)

The expressions P(k+3,m,3,0), P(k+3,m-1,2,1) and P(k+3,m-2,1,2) effectively illustrate the probability of a group of cells with k+3 DSBs and m mis-repaired DSBs successfully repairing 3, 2, or 1 DSB, respectively. Conversely, P(k+3,m-3,0,3), P(k+3,m-2,1,2), and P(k+3,m-1,2,1) signify the likelihood of these cells failing to adequately repair 3, 2, or 1 DSBs when there m-3 are mis-repaired DSBs present. Notably, the chance of successfully repairing three DSBs remains consistent across all cell groups, regardless of the total number of DSBs or mis-repaired DSBs involved. This stable probability is represented by P, while the likelihood of failing to repair 3 DSBs is denoted as 1-P. Therefore, the model presented in Equation (23) can be articulated as follows:

$$\mathbf{N}_{k,m}(\tau + \Delta \tau) = \mathbf{N}_{k,m}(\tau) - \Delta \tau \beta_{1}(k,m) \mathbf{N}_{k,m}(\tau) - \Delta \tau \kappa(k) \mathbf{N}_{k,m}(\tau) + \Delta \tau P(k+3,m,3,0) \kappa(k+3) \mathbf{N}_{k+3,m}(\tau) + \Delta \tau P(k+3,m-3,0,3) \kappa(k+3) \mathbf{N}_{k+3,m-3}(\tau) + \Delta \tau P(k+3,m-1,2,1) \kappa(k+3) \mathbf{N}_{k+3,m-1}(\tau) + \Delta \tau P(k+3,m-2,1,2) \kappa(k+3) \mathbf{N}_{k+3,m-2}(\tau) + \Delta \tau P(k+3,m-2,1,2) \kappa(k+3) \mathbf{N}_{k+3,m-2}(\tau) + \Delta \tau P(k+3,m-1,2,1) \kappa(k+3) \mathbf{N}_{k+3,m-1}(\tau)$$
(24)

Equation (24) models discrete-time updates for $N_{k,m}(\tau)$ assuming that only three DNA DSBs are processed per event. To derive the continuous form, we apply a first-order derivative approximation in Equation (25).

$$\lim_{\Delta \tau \to 0} \frac{\mathbf{N}_{k,m}(\tau + \Delta \tau) - \mathbf{N}_{k,m}(\tau)}{\Delta \tau} = \frac{d\mathbf{N}_{k,m}(\tau)}{d\tau}$$
(25)

Equation (26) builds upon Equation (24) by incorporating additional pathways where one or two DSBs are repaired per step, rather than strictly three. These new transitions introduce the missing k+2 and k+1 terms, making the model more biologically realistic and mathematically comprehensive.

$$\frac{d\mathbf{N}_{k,m}(\tau)}{d\tau} = -\beta_1(k,m)\mathbf{N}_{k,m}(\tau) - \kappa(k)\mathbf{N}_{k,m}(\tau) +
P\kappa(k+3)\mathbf{N}_{k+3,m}(\tau) + (1-P)\kappa(k+3)\mathbf{N}_{k+3,m-3}(\tau) +
P\kappa(k+2)\mathbf{N}_{k+2,m}(\tau) + (1-P)\kappa(k+2)\mathbf{N}_{k+2,m-2}(\tau) + P\kappa(k+1)\mathbf{N}_{k+1,m}(\tau) +
(1-P)\kappa(k+1)\mathbf{N}_{k+1,m-1}(\tau).$$
(26)

As depicted in Figure 1, it is essential to recognize that each of the DSB repair mechanisms necessitates the occurrence of a distinct event. With three unique DSB repair mechanisms at play, we identify a total of nine possible outcomes. Therefore, throughout our study, we carefully define our probability selection in Equation (27) as:

$$P_n \in [1, 0], \text{ for } n = 1, 2, 3.$$
 (27)

The variable P_n is chosen at random from a closed interval comprised of integer values, representing the probabilities of success and failure. These metrics are crucial to our analysis. Equation (28) is more detailed than Equation (26) because it introduces distinct probabilities P_1, P_2P_3 repairing one, two, or three DSBs, replacing the generalized P. This modification enhances biological accuracy by differentiating repair likelihoods and ensures mathematical completeness by properly weighting each repair scenario, leading to a more explicit representation of DNA repair dynamics.

$$\frac{d\mathbf{N}_{k,m}(\tau)}{d\tau} = -\beta_1(k,m)N_{k,m}(\tau) - \kappa(k)\mathbf{N}_{k,m}(\tau) + P_3\kappa(k+3)\mathbf{N}_{k+3,m}(\tau) + (1-P_3)\kappa(k+3)\mathbf{N}_{k+3,m-3}(\tau) + P_2\kappa(k+2)\mathbf{N}_{k+2,m}(\tau) + (1-P_2)\kappa(k+2)\mathbf{N}_{k+2,m-2}(\tau) + P_1\kappa(k+1)\mathbf{N}_{k+1,m}(\tau) + (1-P_1)\kappa(k+1)\mathbf{N}_{k+1,m-1}(\tau),$$
(28)

Equation (20) represents the generalized formulation of Equation (28) by incorporating a summation notation, which consolidates the individual repair probabilities for one, two, and three DSBs into a unified expression. In (28), $\kappa(k)$ and $\beta_1(k,m)$ are given in Equation (4) and (5), defining the rates of DNA repair and cell death following radiation-induced damage. Since DSB repair is not always successful [35]; the probability of a successful repair is expressed as $\sum_{n=1}^{3} P_n \kappa(k+n) \mathbf{N}_{k+n,m}(\tau)$, while the probability of misrepair (incorrect chromosome rejoining) is given $\sum_{n=1}^{3} P_n (1-P_n) \kappa(k+n) \mathbf{N}_{k+n,m-n}(\tau).$

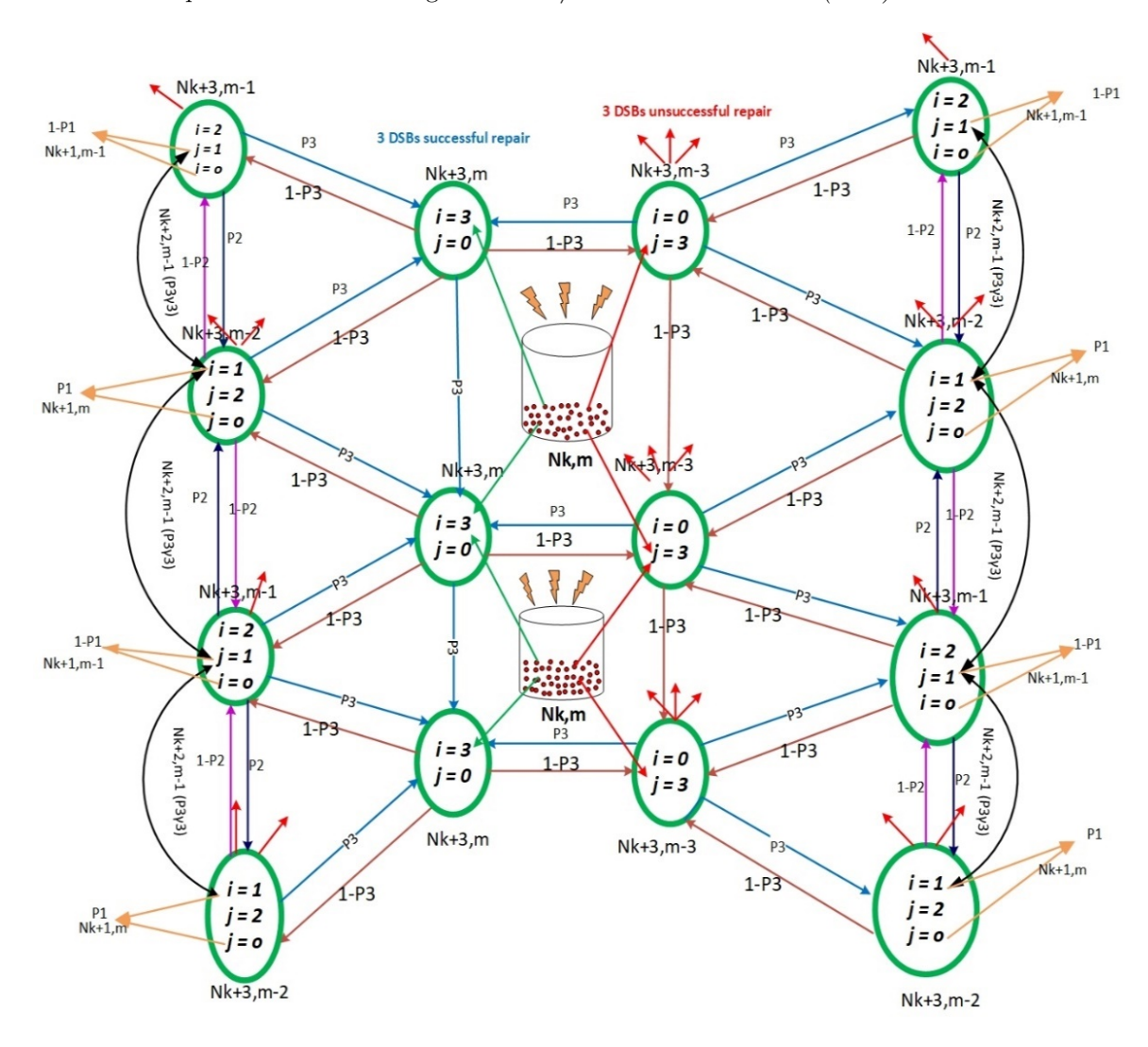


Figure 1: Schematic representation of the modified model illustrating the DSB repair mechanism, incorporating simultaneous repair of up to three DSBs.

In Figure 1, the blue arrows (\rightarrow) illustrate the successful repair of three, two, or one DSBs within the cell population k while the brown arrows (\rightarrow) represent the unsuccessful repair of the same number of DSBs. The probability of successfully repairing three DSBs in this innovative model is indicated by P_3 , with $1-P_3$ reflecting the likelihood of an unsuccessful repair. Additionally, the black arrows (\rightarrow) depict the scenario of one successful and one unsuccessful repair occurring during a two DSB repair process. The orange arrows (\rightarrow) signify either a successful or unsuccessful repair in a single DSB repair pathway (P_1) . Thus, the dark blue arrows (\rightarrow) demonstrate two successful DSB repairs, whereas the purple arrows (\rightarrow) illustrate two unsuccessful repairs within the framework of two DSB repair pathways $(P_2, 1-P_2)$. The notation $N_{k,m}$ designates the cell population, with each green circle symbolizing a distinct subset of cells. After irradiation, the green and red arrows clearly indicate the movement of three successful and three unsuccessful DSB repairs to their respective groups. This schematic diagram goes beyond merely demonstrating the repair of three DSBs at a time; it also accounts

for the potential to repair or not repair two or one DSBs. Accordingly, this allows for a maximum of five DSBs, encompassing all nine possible scenarios. The modifications implemented in this model, drawing on previous research [15, 33], seamlessly integrate the possibilities presented by both original models, ensuring a robust and comprehensive new framework that enhances our understanding of DSB repair mechanisms.

2.3 Initial Conditions

It is widely accepted that the formation of additional DSBs occurs immediately upon irradiation exposure. Building on the research conducted in studies [43, 44], which quantified γ -H2AX phosphorylation foci, an established indicator of DSBs, we assert that the probability of a cell acquiring k DSBs can be effectively modeled by a Poisson distribution, as previously discussed. The likelihood of any specific cell sustaining $k \geq 0$ DSBs is calculated using Equation (2). In the realm of radiation oncology, it is essential to recognize that the values of initially unknown and need to be estimated from cell survival data, alongside other kinetic parameters of the model. In our MATLAB simulations, we generate an array $N_{k,0}(0)$ by sampling from the Poisson distribution with the poissrnd() function. The total cell count in each simulation run is designated as N_0 , while k_{max} indicates the upper limit of DSBs found in our samples. We derive our conclusions by averaging results over multiple iterations. For instance, our analysis involved a cell population size of 20,000 and 20 iterations to ensure robust and reliable findings.

2.4 Limitations

While the structured ODE model offers valuable insights into DNA repair dynamics, it has certain limitations. The primary objective of this study is to enhance the repair rate through the cell survival fraction by modifying the existing model to allow for the simultaneous repair of three DSBs, as previous models only addressed the repair of one DSB at a time [33, 34]. However, we did not consider the cell cycle phase or the effects of low-and high-linear energy transfer (LET) radiation, both of which can influence DNA repair efficiency [42]. Our model assumes a fixed repair rate, but DNA repair processes vary depending on the cell cycle phase. For example, homologous recombination (HR) is predominant during the S and G2 phases, while non-homologous end joining (NHEJ) occurs throughout the cell cycle and is more errorprone [42]. Incorporating cell cycle-dependent repair kinetics in future models could improve biological accuracy. Additionally, our model does not differentiate between low- and high-LET radiation. High-LET radiation such as alpha particles, carbon ions among others creates complex DNA damage clusters that are more challenging to repair than damage caused by low-LET radiation like X-rays and gamma rays [32,33]. Future enhancements could include integrating radiation quality factors to better account for repair efficiencies across different LET exposures. Lastly, although our model expands the traditional framework by permitting the concurrent repair of multiple DSBs, it does not consider the influence of cellular microenvironments, such as oxidative stress, cytokine signaling, and indirect radiation-induced DNA damage in bystander [36]. Future work could incorporate stochastic elements to capture these interactions more accurately. Despite these limitations, our modified model represents a significant advancement in understanding DNA repair dynamics by allowing the concurrent repair of three DSBs. Future research should aim to incorporate cell cycle effects, LET-dependent damage characteristics, and stochastic modeling of microenvironmental influences to further enhance the model's applicability.

3 Results and Discussion

3.1 Simulation results

We begin our investigation by establishing the initial conditions based on critical kinetic parameters $\alpha_1, \alpha_2, P, V_{max}, K_M, \delta$ and the radiation dose D, as detailed in the preceding section. Once we define k_{max} , we will adeptly solve a set of linear equations represented by matrix N, which is derived from the k_{max} value. The matrix, with dimensions of $Q \times Q$, is calculated using the formula $Q = \frac{(k_{max} + 1)(k_{max} + 2)}{2}$, as outlined in Equations (3) and Equation (28). To tackle the problem effectively, we employed MATLAB to develop a robust algorithm consisting of five sequential steps designed to accurately calculate the survival fraction of cells. The methodology is structured as follows:

- 1. Initially, we generate a set of initial conditions, denoted as N(0) along with a specified radiation dose, D. This dosage is crucial as it allows us to calculate the mean value, μ , which is key to generating the initial conditions [36].
- 2. Subsequently, we explore the system's solution over a time frame of $\tau = \Gamma$, where Γ is set at 24 hours which indicate the maximum time for-cell cycle [42]. This time period is strategically chosen to ensure that repair processes are completed, as extensive research shows that cellular recovery from radiation is typically finalized within 24 hours [42]. Moreover, studies [42] reveal that over 80% of DSBs are effectively repaired within 12 hours post-exposure.
- 3. Following this, we proceed to calculate the survival fraction of cells, represented as $S = \frac{\sum_{k,m} \mathbf{N}_{k,m}(\Gamma)}{\sum_{k,m} \mathbf{N}_{k,m}(0)} \quad [35,37].$
- 4. We then plot the natural logarithm of the survival fraction, denoted as $\ln S$, against the dose D. To accommodate the variability originating from initial conditions, we repeat steps 1-3 twenty-five times to achieve an average value for $\ln S$. This step culminates in a single data point corresponding to a specific dose D. To create a compelling survival curve, it is essential to repeat these steps and compute the average $\ln S$ for each dosage D.
- 5. Once we have gathered all necessary data, we fit the LQ relation to the results.

In our study, we present a total of 25 simulated data points, making use of the parameter values: $\delta = 0.818$, $\alpha_1 = 1.5$, $\alpha_2 = 0.002$, P = 0.95, $V_{max} = 1$ and $K_M = 3$. These parameters were carefully chosen, adhering to the recommended ranges detailed in sources [33] as shown in Table 1. Research [45] indicates that the optimal value rests between 2-40 per Gray per cell, with variations depending on the cell type. To derive values for α_2 , investigators [46] utilized survival data from Chinese hamster ovary (CHO) cells, establishing that α_2 lies between 0 and

0.005 per hour, while α_1 is estimated to range from 0.0277 and 20.79 per hour. Table 2 summarizes these value ranges for V_{max} and K_M , as noted by [46]. We compiled six experimental survival datasets from a range of cell lines exposed to various radiation types [39]. Figure 2 presents averaged survival data points (o) from 25 model iterations, fitted to an LQ relation, showcased by a smooth curve. The strong fit corroborates our understanding of repair, misrepair, and cell death processes, validating the LQ relation. Figure 3 compares our simulation results with those of the existing one DSB repair model outlined in [33], While both simulations involve different parameters from Tables 1 and Table 2 respectively, it is evident that our findings culminate in a marked improvement in cell viability. Specifically, Figure 2 reveals a cell survival fraction of 64.18% at a maximum dose of 12 Gray, while Figure 3 indicates only 27.79% survival based on the existing model. This stark contrast highlights that more cells remained viable using our modified approach. However, further investigation is needed by incorporating biological factors such as the cell cycle, radiation types, and the microenvironment, which may enhance outcomes [42].

 Table 1: Lower Bound and Upper Bound for the Parameter of the Models

Parameter	Lower Bound	Upper Bound	Reference
δ	0.0001	40	[28]
α_1	0.0277	20.79	[28]
α_2	0.0001	0.005	[28]
P	0	1	[33]
V_{max}	0.1	3	[28]
K_{M}	0.0001	5	[28]

Table 2: Parameter Values of the Models [33]

Parameter	Descriptions	Value	
δ	Radiosensitivity of cells	$2 Gh^{-1}$	
α_1	Mis-repair rate constant	$1.5 h^{-1}$	
α_2	Lethal binary mis repair rate constant	$0.001 \ h^{-1}$	
P	Probability of cell with k and m repair	0.95	
	correctly and v incorrectly at a unit time		
V_{max}	Maximum repair rate	$1h^{-1}$	
K_M	Michaelis -Menten Constant, the number of	$\frac{1}{2}$ μM	
	DSBs repair rate is half of V_{max}	$3 \mu M$	

Besides, in Figure 2, we also present compelling simulation results from one administration of dose D (represented by a circle) at $\tau=24$ hours. These results were achieved using carefully selected parameter values: $\delta=0.818$, $\alpha_1=1.5$, $\alpha_2=0.002$, P=0.95, V_{max} and $K_M=3$. To ensure the simulation data aligns with established empirical principles, we tailored it to follow the LQ relationship expressed by the equation $\ln S=-0.0223D-0.0012D^2$, illustrated by a thin line. Notably, the model parameters were refined to $\alpha_{model}=0.0023\pm9.9307\times10^{-6}$ and $\beta_{model}=0.0012\pm9.9307\times10^{-6}$. This adjustment enhances the reliability of our findings and underscores the significance of the observed relationships.

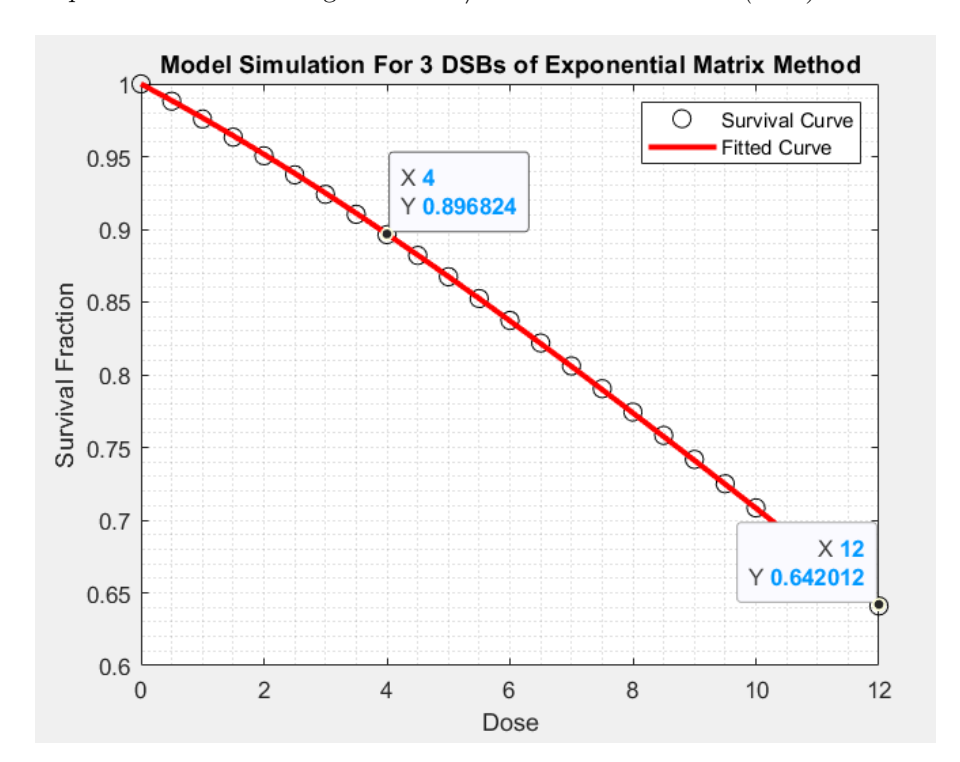


Figure 2: The modified model can simultaneously repair three DSBs using the Exponential Matrix Method, resulting in a higher cell survival rate plotted against radiation dose. This confirms the importance of multiple DSB repair mechanisms for predicting radiation-induced cell survival.

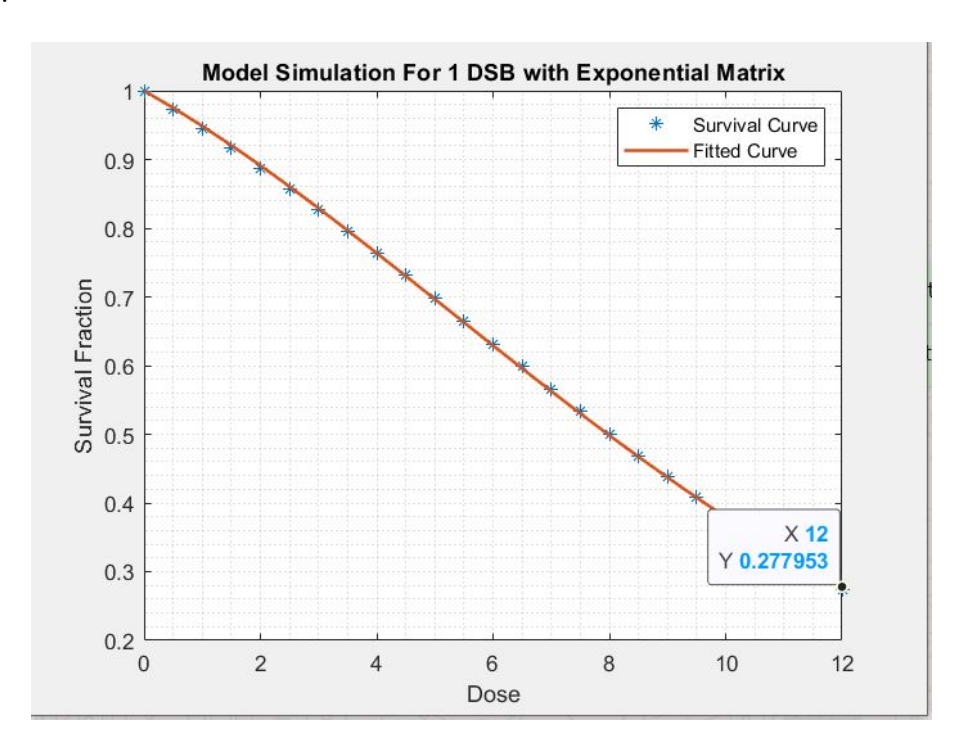


Figure 3: The existing model, which assumes only one DSB can be repaired at a time, shows a significantly lower survival fraction at higher radiation doses, highlighting the limitations of single-DSB repair assumptions and the need to consider simultaneous DNA repair processes.

In addition, in Figure 3, we present compelling evidence from a simulation of a single dose administration (designated by an asterisk) at $\tau=24$ hours. This simulation utilizes a carefully selected set of parameters: $\delta=2, \alpha_1=1.5, \alpha_2=0.001, P=0.95, V_{max}=1$ and $K_M=3$. Notably, the simulation data has been meticulously calibrated to conform to the established linear-quadratic (LQ) relationship, represented as $\ln S=-0.0478D-0.0049D^2$ (as depicted by the solid line). The parameters for our model are defined as, with $\alpha_{model}=0.0478\pm1.4835\times10^{-4}$ and $\beta_{model}=0.0049\pm1.4835\times10^{-4}$, underscoring the robustness of our findings.

To further evaluate the accuracy of our modified model, we compared its predicted survival fractions with experimental survival data [40], as illustrated in Figure 4. The experimental data were analyzed using the LQ model [34], which allows for a direct comparison with the simulated survival fraction values [34,35]. The fitted curve (shown as a red line) closely follows the trend of the experimental data points (marked by blue stars), indicating that the model's predictions align well with actual biological outcomes. This agreement suggests that incorporating the ability to repair three DSBs simultaneously offers a more explicit representation of DNA damage repair dynamics in cells exposed to radiation. Furthermore, at a dose of 4 Gy, the survival fraction predicted by the modified model in Figure 2 remains within the range observed in the experimental datasets in Figure 4, reinforcing the biological plausibility of our approach. This comparison shows that the new model not only improves theoretical survival fractions but also maintains consistency with empirically validated survival trends. However, future work could further refine this approach by incorporating additional experimental datasets to evaluate variations across different cell types and radiation qualities and quantities. This significant improvement can be attributed to enhancements in the existing model, particularly the incorporation of repair processes for three DSBs. Additionally, the strategic selection of parameter values $\delta = 0.818$ and $\alpha_2 = 0.002$, has greatly amplified the survival proportion [36]. Such progress represents a noteworthy achievement, not only for our model but also for advancing other radiobiological models focused on survival fractions. The survival percentages presented were derived by multiplying the survival fraction at the maximum dose by 100, as given in this study, emphasizing the rigor of our approach.

3.2 Biological Implications and Challenges

One of the most intriguing areas of the DNA damage response that warrants further investigation is the impact of bystander effects on DNA repair efficiency. Our research primarily emphasizes bystander cells which are not directly subjected to irradiation but experience the influence of signals from their neighboring irradiated counterparts. It's fascinating to note that irradiated cells can release signaling molecules, including cytokines and reactive oxygen species (ROS), which may either enhance or inhibit DNA repair in adjacent cells. The degree to which these intercellular signals can modulate DNA repair mechanisms is a captivating question and could significantly affect overall cell survival [26]. Our findings reveal that when multiple DSBs are repaired simultaneously, there is a markedly higher survival fraction compared to models permitting only single DSB repairs [15, 33, 36]. This indicates that cells possess robust mechanisms to manage clustered DNA damage more efficiently than previously understood. However, it's important to consider that at higher radiation doses, we see an increased likelihood of repair saturation, which can lead to misrepair events [33]. This agrees with experimental evidence that significant DSB clustering overwhelms repair pathways, increasing genomic instability.

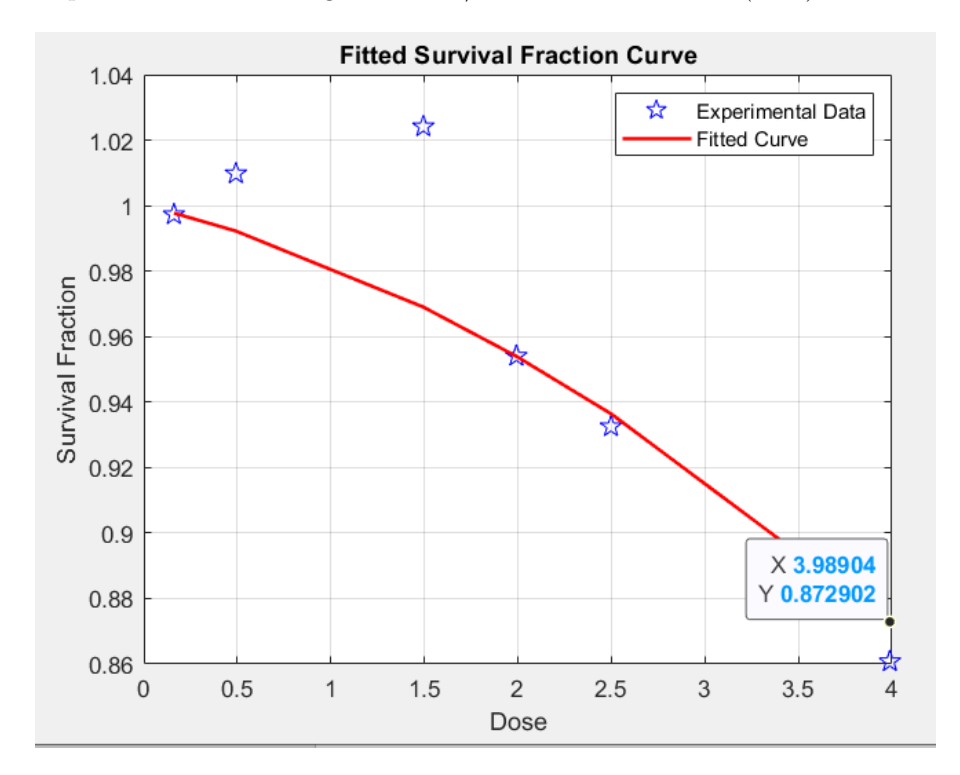


Figure 4: Fitted survival fraction curve based on experimental data of Human Colon Carcinoma cells (HCT 116) irradiated with 150 MeV proton beams treated with gold nanoparticles (AuNPs) [40]. The experimental data points (blue stars) represent measured survival fractions at different radiation doses, while the fitted curve (red line) follows the expected trend using the LQ model. This comparison validates the model's ability to approximate experimentally observed survival trends, demonstrating the impact of AuNPs on radiation response.

While our model shows an enhanced survival fraction under this multi-DSB repair framework, it's crucial to explore other possible explanations. Differences in factors like the activation of repair pathways, variations in bystander-mediated signaling, or changes in chromatin accessibility that influence damage recognition could also play a role. Future studies may benefit from incorporating stochastic modeling to better understand how these variables influence DNA repair efficiency in populations exposed to radiation. Despite the complexities we face, our results offer an exciting new perspective on the mechanics of radiation-induced DNA damage repair, particularly regarding bystander cell interactions. By adapting traditional models to accommodate multiple DSB repairs, this study enhances our understanding of cell survival dynamics in radiation exposure. Future research should focus on integrating dose-dependent bystander responses and stochastic modeling of intercellular communication to refine our predictions of DNA repair and survival outcomes in irradiated populations. We are optimistic about the potential these findings hold for advancing our understanding of DNA damage response mechanisms and their implications for health and disease.

4 Conclusion

DSBs are a major consequence of irradiation, with improper repair potentially leading to severe health implications, including cancer. This study refines existing models by introducing a framework that enables the simultaneous repair of three DSBs, improving our understanding of cellular response to radiation-induced DNA damage. Our simulation results, validated against experimental data, indicate a significant improvement in cell survival compared to previous models focusing solely on single-DSB repair. By incorporating additional repair pathways, our approach offers a more biologically relevant representation of DSB dynamics. Future work will focus on extending the model by integrating cell cycle-dependent repair mechanisms and refining parameter estimation through further sensitivity analysis. This research contributes to the ongoing development of predictive models for DNA repair, with potential applications in radiation therapy and cellular damage mitigation.

Acknowledgments

The authors would like to acknowledge the financial support from the Universiti Teknologi Malaysia through the UTM encouragement research grant scheme, grant number Q.J130000.3854.20J20.

References

- [1] Sadoughi, F., Hallajzadeh, J., Asemi, Z., Mansournia, M. A., Alemi, F. and Yousefi, B. Signaling pathways involved in cell cycle arrest during the DNA breaks. DNA Repair (Amst). Elsevier B.V.; 2021. https://doi.org/10.1016/j.dnarep.2021.103047
- [2] Heeran, A. B., Berrigan, H. P. and O'Sullivan, J. The Radiation-Induced Bystander Effect (RIBE) and its Connections with the Hallmarks of Cancer. Radiat Res. Radiation Research Society; 2019. p. 668-79. https://doi.org/10.1667/RR15489.1
- [3] Deycmar, S., Faccin, E., Kazimova, T., Knobel, P. A., Telarovic, I., Tschanz, F., et al. The relative biological effectiveness of proton irradiation in dependence of DNA damage repair. Br J Radiol. 2020;93. https://doi.org/10.1259/bjr.20190494
- [4] Mladenov, E., Mladenova, V., Stuschke, M. and Iliakis, G. New Facets of DNA Double Strand Break Repair: Radiation Dose as Key Determinant of HR versus c-NHEJ Engagement. Int J Mol Sci. 2023;24:14956. https://doi.org/10.3390/ijms241914956
- [5] Li, L., Guan, Y., Chen, X., Yang, J. and Cheng, Y. DNA Repair Pathways in Cancer Therapy and Resistance. Front Pharmacol. 2021;11. https://doi.org/10.3389/fphar. 2020.629266
- [6] Song, C. W., Glatstein, E., Marks, L. B., Emami, B., Grimm, J., Sperduto, P. W., et al. Biological Principles of Stereotactic Body Radiation Therapy (SBRT) and Stereotactic Radiation Surgery (SRS): Indirect Cell Death. Int J Radiat Oncol Biol Phys. Elsevier Inc.; 2021;110:21-34. https://doi.org/10.1016/j.ijrobp.2019.02.047

- [7] Kyriakou, I., Sakata, D., Tran, H. N., Perrot, Y., Shin, W. G., Lampe, N., et al. Review of the Geant4-DNA Simulation Toolkit for Radiobiological Applications at the Cellular and DNA Level. Cancers (Basel). 2021;14:35. https://doi.org/10.3390/cancers14010035
- [8] Cordoni, F. G. A spatial measure-valued model for radiation-induced DNA damage kinetics and repair under protracted irradiation condition. J Math Biol. 2024;88:21. https://doi.org/10.1007/s00285-024-02046-3
- [9] Sakata, D., Belov, O., Bordage, M. C., Emfietzoglou, D., Guatelli, S., Inaniwa, T., et al. Fully integrated Monte Carlo simulation for evaluating radiation induced DNA damage and subsequent repair using Geant4-DNA. Sci Rep. 2020;10:20788. https://doi.org/10.1038/s41598-020-75982-x
- [10] Ingram, S. P., Henthorn, N. T., Warmenhoven, J. W., Kirkby, N. F., Mackay, R. I., Kirkby, K. J., et al. Hi-C implementation of genome structure for in silico models of radiation-induced DNA damage. PLoS Comput Biol. 2020;16:e1008476. https://doi.org/10.1371/journal.pcbi.1008476
- [11] Das, D., Li, J., Cheng, L., Franco, S. and Mahairaki, V. Human Forebrain Organoids from Induced Pluripotent Stem Cells: A Novel Approach to Model Repair of Ionizing Radiation-Induced DNA Damage in Human Neurons. Radiat Res. 2020;194:191. https://doi.org/10.1667/RR15567.1
- [12] Barragan-Montero, A., Bibal, A., Dastarac, M. H., Draguet, C., Valdes, G., Nguyen, D., et al. Towards a safe and efficient clinical implementation of machine learning in radiation oncology by exploring model interpretability, explainability and data-model dependency. Phys Med Biol. Institute of Physics; 2022;67.https://doi.org/10.1088/1361-6560/ac678a
- [13] Nisar, K. S., Farman, M., Zehra, A. and Hincal, E. Numerical and analytical study of fractional order tumor model through modeling with treatment of chemotherapy. International Journal of Modelling and Simulation. Taylor and Francis Ltd.; 2024; https://doi.org/10.1080/02286203.2024.2327659
- [14] Huang, R. and Zhou, P. K. DNA damage repair: historical perspectives, mechanistic pathways and clinical translation for targeted cancer therapy. Signal Transduct Target Ther. Springer Nature; 2021. https://doi.org/10.1038/s41392-021-00648-7
- [15] Mohd Siam, F. and Hanis Nasir, M. Derivation of Repair and Mis-Repair DNA Double-Strand Breaks (DSBs) Model: A Case with Two Simultaneously DSBs Repair Condition. JOURNAL OF SCIENCE AND TECHNOLOGY [Internet]. 2020;12:1-6. https://doi.org/10.30880/jst.2020.12.01.001
- [16] Taleei, R., Rahmanian, S. and Nikjoo, H. Modelling Cellular Response to Ionizing Radiation: Mechanistic, Semi-Mechanistic, and Phenomenological Approaches a Historical Perspective. Radiat Res. 2024;202. https://doi.org/10.1667/RADE-24-00019.1

- [17] Wang, J., Ma, W., Si, C., Zhang, M., Qian, W., Park, G., et al. Exosome-mediated miR-4655-3p contributes to UV radiation-induced bystander effects. Exp Cell Res. Elsevier Inc.; 2022;418.https://doi.org/10.1016/j.yexcr.2022.113247
- [18] Rezaei, M., Esmailzadeh, A. and Shanei, A. Bystander Effect of Therapeutic Ultrasound in the Presence of Cisplatin: An in Vitro Study on Human Melanoma Cells. J Biomed Phys Eng. Shiraz University of Medical Sciences; 2023;13:433-442. https://doi.org/10. 31661/jbpe.v0i0.2105-1337
- [19] Gonon, G., de Toledo, S. M., Perumal, V., Jay-Gerin, J. P. and Azzam, E. I. Impact of the redox environment on propagation of radiation bystander effects: The modulating effect of oxidative metabolism and oxygen partial pressure. Mutat Res Genet Toxicol Environ Mutagen. Elsevier B.V.; 2022;883-884. https://doi.org/10.1016/j.mrgentox.2022.503559
- [20] López-Gil, L., Pascual-Ahuir, A. and Proft, M. Genomic Instability and Epigenetic Changes during Aging. Int J Mol Sci. Multidisciplinary Digital Publishing Institute (MDPI); 2023. https://doi.org/10.3390/ijms241814279
- [21] Jenkins, S. V., Johnsrud, A. J., Dings, R. P. M. and Griffin, R. J. Bystander Effects in Spatially Fractionated Radiation Therapy: From Molecule To Organism To Clinical Implications. Semin Radiat Oncol. W.B. Saunders; 2024. p. 284-291.https://doi.org/ 10.1016/j.semradonc.2024.05.004
- [22] Shimura, T. Mitochondrial Signaling Pathways Associated with DNA Damage Responses. Int J Mol Sci. Multidisciplinary Digital Publishing Institute (MDPI); 2023. https://doi.org/10.3390/ijms24076128
- [23] Hou, G., Li, J., Liu, W., Wei, J., Xin, Y. and Jiang, X. Mesenchymal stem cells in radiation-induced lung injury: From mechanisms to therapeutic potential. Front Cell Dev Biol. Frontiers Media S.A.; 2022. https://doi.org/10.3389/fcell.2022.1100305
- [24] Wiedemann, J., Coppes, R. P. and van Luijk, P. Radiation-induced cardiac side-effects: The lung as target for interacting damage and intervention. Front Oncol. Frontiers Media S.A.; 2022. https://doi.org/10.3389/fonc.2022.931023
- [25] Tong, J. Biophoton signaling in mediation of cell-to-cell communication and radiation-induced bystander effects. Radiat Med Prot. Elsevier B.V.; 2024. https://doi.org/10.1016/j.radmp.2024.06.004
- [26] Jassi, C., Kuo, W. W., Kuo, C. H., Chang, C. M., Chen, M. C., Shih, T. C., et al. Mediation of radiation-induced bystander effect and epigenetic modification: The role of exosomes in cancer radioresistance. Heliyon. Elsevier Ltd; 2024. https://doi.org/10. 1016/j.heliyon.2024.e34460
- [27] Liao, K. L., Wieler, A. J. and Gascon, P. M. L. Mathematical modeling and analysis of cancer treatment with radiation and anti-PD-L1. Math Biosci. Elsevier Inc.; 2024;374. https://doi.org/10.1016/j.mbs.2024.109218

- [28] Rashid, H., Siam, F. M., Maan, N., Nordiana, W., Rahman, W. A. and Nasir, M. H. Mathematical Model of the Generation of Radiation-induced DNA Double-strand Breaks and Misrepair Cells by Direct and Indirect Action. *Malaysian Journal of Fundamental and Applied Sciences*. 2022.
- [29] Gyllingberg, L., Birhane, A. and Sumpter, D. J. T. The lost art of mathematical modelling. Math Biosci. Elsevier Inc.; 2023;362. https://doi.org/10.1016/j.mbs.2023.109033
- [30] Arnould, C., Rocher, V., Finoux, A-L., Clouaire, T., Li, K., Zhou, F., et al. Loop extrusion as a mechanism for formation of DNA damage repair foci. Nature. 2021;590:660-665. https://doi.org/10.1038/s41586-021-
- [31] Chen, J., Ma, W., Ma, Y. and Yang, G. Double-Strand Break Clustering: An Economical and Effective Strategy for DNA Repair.
- [32] De Falco, M. and De Felice, M. Take a Break to Repair: A Dip in the World of Double-Strand Break Repair Mechanisms Pointing the Gaze on Archaea. Int J Mol Sci. 2021;22:13296. https://doi.org/10.3390/ijms222413296
- [33] Siam, F. M., Grinfeld, M., Bahar, A., Rahman, H. A., Ahmad, H. and Johar, F. A mechanistic model of high dose irradiation damage. Math Comput Simul. Elsevier B.V.; 2018;151:156-168. https://doi.org/10.1016/j.matcom.2016.02.007
- [34] Rashid, H., Siam, F. M., Maan, N., Nordiana, W. and Rahman, A. Ionizing Radiation Effects Modelling in Cells Population with Gold Nanoparticles. Malaysian Journal of Fundamental and Applied Sciences. 2021.
- [35] Muhamad Hanis bin Mohd Nasir. Modelling of Ionizing Radiation Effects Towards Bystanders Cells [Thesis]. [Johor]: Universiti Teknologi Malaysia; 2018.
- [36] Siam, F. M. and Nasir, M. H. Mechanistic Model of Radiation-Induced Bystander Effects to Cells using Structured Population Approach [Internet]. MATEMATIKA. 2018. www.matematika.utm.my
- [37] Fuaada Mohd Siam. Modelling effects of ionising radiation [PhD Thesis]. [Glasgow, UK]: University of Strathclyde; 2014.
- [38] Kutuva, A. R., Caudell, J. J., Yamoah, K., Enderling, H., Zahid, M. U. Mathematical modeling of radiotherapy: impact of model selection on estimating minimum radiation dose for tumor control. Front Oncol. Frontiers Media SA; 2023;13.https://doi.org/10.3389/fonc.2023.1130966
- [39] Abdul Rashid, R., Zainal Abidin, S., Khairil Anuar, M. A., Tominaga, T., Akasaka, H., Sasaki, R., et al. Radiosensitization effects and ROS generation by high Z metallic nanoparticles on human colon carcinoma cell (HCT116) irradiated under 150 MeV proton beam. OpenNano. Elsevier Inc; 2019;4. https://doi.org/10.1016/j.onano.2018.100027

- [40] van Leeuwen, C. M., Oei, A. L., Crezee, J., Bel, A., Franken, N. A. P., Stalpers, L. J. A., et al. The alfa and beta of tumours: A review of parameters of the linear-quadratic model, derived from clinical radiotherapy studies. Radiation Oncology. BioMed Central Ltd.; 2018. https://doi.org/10.1186/s13014-018-1040-z
- [41] Haym Benaroya and Seon Mi Han. Probability Models in Engineering and Science. L. L. Faulkner, editor. London: CRC PressTaylor & Francis Group 6000 Broken Sound Parkway NW, Suite 300Boca Raton, FL 33487-2742; 2005.
- [42] Mohseni-Salehi, F. S., Zare-Mirakabad, F., Sadeghi, M. and Ghafouri-Fard, S. A Stochastic Model of DNA Double-Strand Breaks Repair Throughout the Cell Cycle. Bull Math Biol. Springer; 2020;82. https://doi.org/10.1007/s11538-019-00692-z
- [43] Penninckx, S., Pariset, E., Cekanaviciute, E. and Costes, S. V. Quantification of radiation-induced DNA double strand break repair foci to evaluate and predict biological responses to ionizing radiation. NAR Cancer. Oxford University Press; 2021;3. https://doi.org/10.1093/narcan/zcab046
- [44] Beinke, C., Port, M. and Scherthan, H. Postirradiation temperature influences DSB repair and dicentric chromosome formation-potential impact for dicentric chromosome analysis in interlaboratory comparisons. Radiat Prot Dosimetry. 2023;199:1485-1494. https://doi.org/10.1093/rpd/ncad128
- [45] Abolfath, R., Khalili, M., Senejani, A. G., Kodery, B. and Ivker, R. The Dependence of Compensation Dose on Systematic and Random Interruption Treatment Time in Radiation Therapy. Onco. MDPI AG; 2022;2:264-281. https://doi.org/10.3390/onco2030015
- [46] Pfuhl, T., Friedrich, T. and Scholz, M. Prediction of Cell Survival after Exposure to Mixed Radiation Fields with the Local Effect Model. Radiat Res. 2019;193:130. https://doi.org/10.1667/RR15456.1